ARKIV FÖR FYSIK Band 17 nr 21

Communicated 25 November 1959 by OSKAR KLEIN and IVAR WALLER

A study of some temperature effects on the phonons in aluminium by use of cold neutrons

By K.-E. LARSSON, U. DAHLBORG, S. HOLMRYD

With 12 figures in the text

SUMMARY

Using the cold neutron scattering technique about 300 phonons have been determined in a single aluminium crystal at room temperature to define 10 pairs of dispersion curves. Investigations have been made of the variation of frequencies, phonon line widths and multi-phonon spectra in the temperature range $293 \leqslant T \leqslant 932°K$. For a particular direction in the crystal lattice it is shown that the frequencies vary about 15 % over this temperature range. The line widths are of such a magnitude that the derived phonon mean free paths vary from about 5 phonon wave lengths at 600°K to about 1.5 phonon wave lengths at 930°K. The observed multi-phonon spectra are found to agree with calculated differential cross sections in the incoherent approximation.

I. Introduction

As indicated by theoretical work by Waller and Fröman [1], and Placzek and Van Hove [2] slow neutrons should be a useful tool to investigate the properties of the phonons in solids. Later successful experiments by Brockhouse *et al.*, and Hughes and Palevsky *et al.* have shown that the careful analysis of the energy and angular distribution of the slow neutrons scattered inelastically in fact makes it possible to study single phonon processes and determine the dispersion relations $\omega = \omega(\mathbf{q})$ in the case of coherent inelastic scattering [3] and to derive the vibrational frequency spectrum in the case of incoherent inelastic scattering [4]. In general the inelastic scattering processes are in the coherent case governed by the energy and momentum conservation laws

$$E_{\text{out}} - E_{\text{in}} = \epsilon \hbar \sum_{i=1}^{m} \omega_i \qquad \begin{array}{l} \epsilon = +1 \text{ for energy gain} \\ \epsilon = -1 \;\;,, \qquad ,, \quad\; \text{loss} \end{array} \tag{1 a}$$

$$\mathbf{k}_{\text{out}} - \mathbf{k}_{\text{in}} = \boldsymbol{\tau} + \sum_{i=1}^{m} \mathbf{q}_i \tag{1 b}$$

where $E = \hbar^2 k^2/2m$ represents the neutron energy, the $\mathbf{q}_i$:s are the phonon wave vectors belonging to the frequencies ω_i. As long as the temperature of the single crystal under study is lower than the Debye temperature, θ_D, of the crystal, the most pronounced inelastic coherent scattering effect is by far the single phonon scattering with $m = 1$.

At higher crystal temperatures, however, the multi-phonon scattering becomes increasingly important, the cross section for these processes increasing rapidly with temperature [5]. Disregarding a minor effect of singularities in the two-phonon scattering [6] ($m = 2$) the neutron spectra expected from higher phonon scattering ($m > 2$) are continuous without any pronounced maxima and minima as in the case of one-phonon scattering. This should at least be true for the incoherent scattering. In the case of coherent inelastic scattering there might possibly occur some weak intensity maxima and minima in the scattering picture for the two-phonon case but for three-phonon and higher processes any sharp structure should be washed out by the averaging effect taking place in the scattering.

The conclusion of these theoretical predictions is that there is a good chance that the technique of the inelastic coherent scattering of slow neutrons could be used even at high crystal temperatures, $T > \theta_D$, to give information on the single phonons just because of the pronounced discontinuous nature of the one-phonon processes and because of the continuous nature of the multi-phonon scattering processes.

With these ideas in mind a study of the lattice vibrations in an aluminium single crystal from room temperature, 293°K, up to the melting pint, 932°K, was undertaken, using the cold neutron scattering technique. The reason why aluminium was chosen as sample was that its cross section is all coherent, which is of particular importance if one wants to avoid complications in the interpretation of the continuous multi-phonon spectra obtained at higher sample temperatures.

II. Experimental method

a. General

In general the experimental problem encountered in inelastic neutron scattering studies is twofold: first to produce a monochromatic incoming neutron beam to define $\mathbf{k}_{\text{in}}$ of equation (1) and second to perform an angular and energy analysis of the scattered neutrons defining the vectors $\mathbf{k}_{\text{out}}$. In the present experiment the cold neutron technique using a beryllium filter to produce a spectrum with the well known cut off at 3.95 Å was used to define the ingoing neutron wave length [3, 4, 7, 8]. The disadvantage with this technique is the large width of this spectrum—the full width at half maximum about 1 Å—which in general leaves the question open as to what the effective ingoing neutron energy actually is. Particularly this might be serious for small energy gain processes, where this gain is only of the order of $(1\text{–}2) \cdot E_{\text{in}}$. The intensity transmitted by a filter is, however, very high, about 1 % of the total thermal neutron flux in a reactor beam being transmitted if the filter is cooled to liquid nitrogen temperature [7]. Using a special technique of interpretation of data it is possible to overcome the difficulty presented by the width of the spectrum as will be discussed in the next section.

Using the filter technique it is also possible to work with large samples, a fact which of course improves the scattered intensity. In the present experiment a beam area of 5×10 cm^2 was utilized and the single aluminium crystal used had a diameter of 6.5 cm and a length of ~ 12 cm. This is an advantage as far as study of single phonon processes is concerned. However, in the study of the broad multi-phonon scattered spectra, the multiple scattering effect in big samples might be of such a magnitude that the use of smaller samples is unavoidable.

The complete experimental set up involving the filter, chopper and time-of-flight

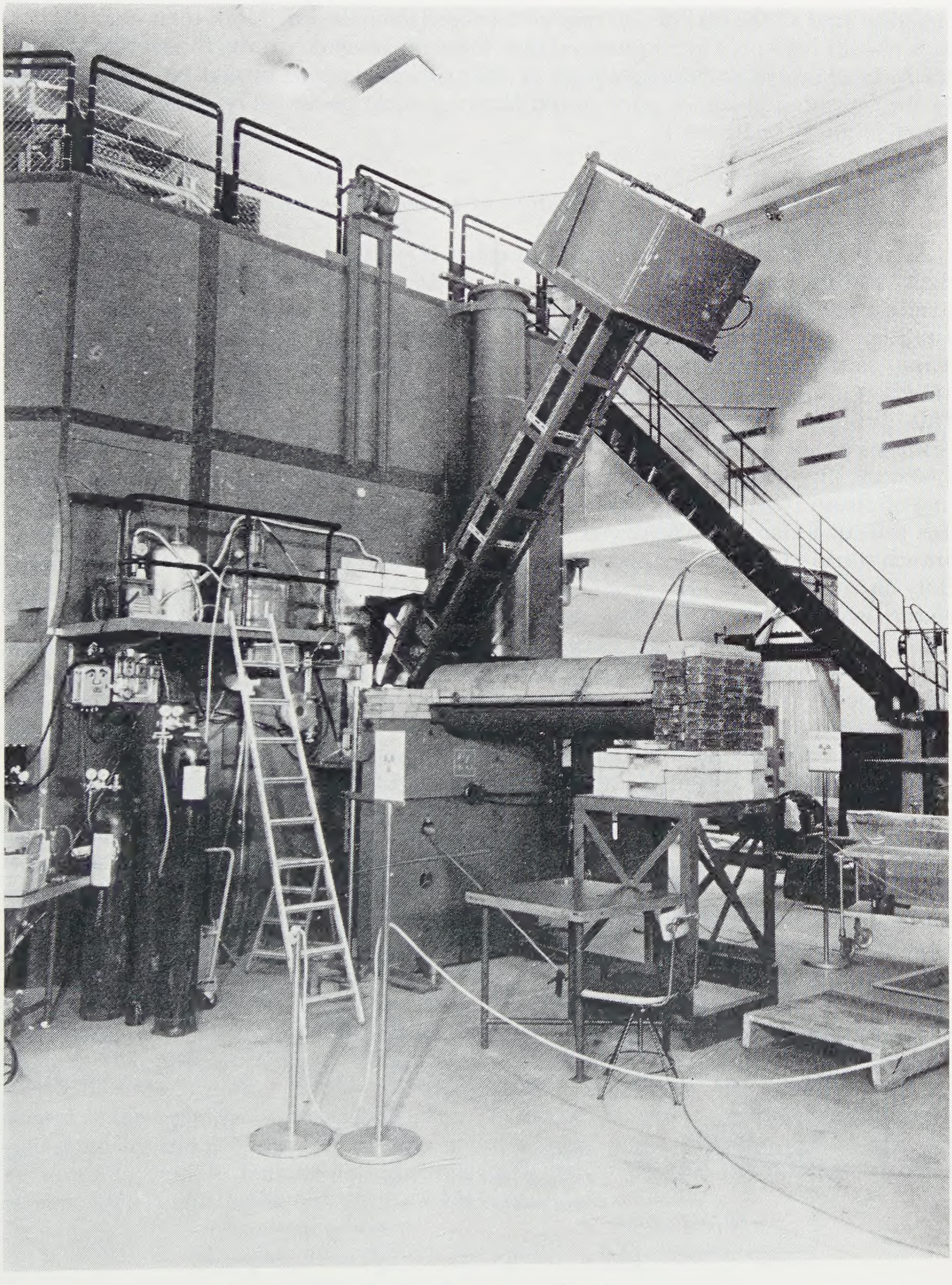

Fig. 1. Spectrometer set up at the Stockholm reactor.

analyzer used at the Stockholm reactor has been described in detail elsewhere [9, 10], so it should here only be emphasized that the arrangement permits the scattered spectra to be observed at various angles of observation between 0° and 90° with respect to the incoming beam. A photograph showing some essential parts of the spectrometer is given in figure 1.

b. Interpretation of scattered spectra

As just mentioned the main problem using the filter technique is to associate the right ingoing wave length with any particular scattered intensity maximum. To simplify the generally rather complicated shape of the scattered spectra all the observations to be described in the following were made in a principal plane, the 001 plane, of the aluminium single crystal, i.e. the crystal was oriented with its [001] direction horizontally, coinciding with the axis of rotation of the spectrometer arm. This arrangement simplifies the observations because one of the "transverse" branches (more correctly: one of the low frequency branches) is associated with zero scattering intensity, leaving us in general with two intensity maxima for any direction of observation and any crystal orientation as long as the observation is made in this principal plane. The observed branches then are one high and one low frequency branch corresponding to vibrations of longitudinal and transverse nature respectively. Only in directions of high symmetry these vibrations are pure. A typical scattering picture obtained at room temperature for a 90° angle of observation is shown in figure 2. As shown in this figure the ingoing broad spectrum might be reproduced in two ways by one-phonon scattering (the multi-phonon scattering is at room temperature associated with a very low cross section) either (a) all the scattered intensity is concentrated in one narrow peak, (b) the scattered spectrum very nearly reproduces the shape of the ingoing cold neutron spectrum including the sharp cut off. In certain directions other intermediate and complicated alternatives might occur, but these

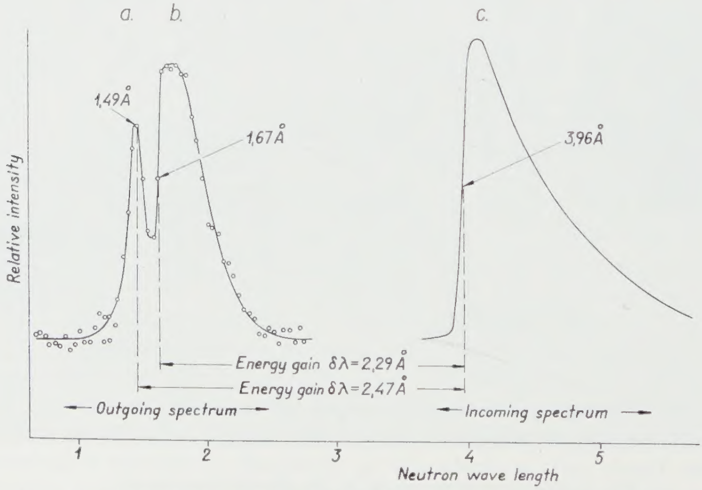

Fig. 2. Typical scattered spectrum obtained experimentally. a. The one-phonon scattering results in a narrow maximum. b. The one-phonon scattering results in a broad maximum with a sharp front edge. c. The incoming spectrum.

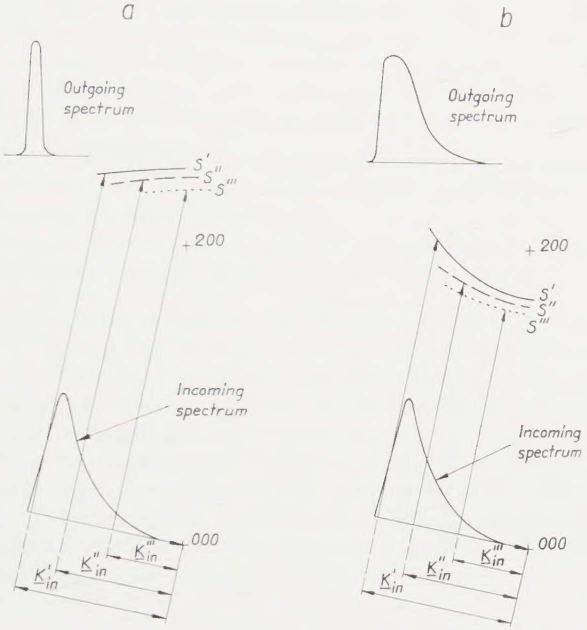

Fig. 3. Explanation of the spectrum given in figure 2. a. Narrow maximum formation. b. Broad maximum formation. Ingoing spectrum given along the vector $\mathbf{k}_{\text{in}}$.

are the principal shapes of the scattered spectra. To explain these two important scattering pictures the scattering surfaces generated for different $\mathbf{k}_{\text{in}}$ vectors are given in figure 3.[1] In general each incoming neutron energy or wave vector $\mathbf{k}_{\text{in}}^{(i)}$ corresponds to a particular scattered neutron energy or wave vector $\mathbf{k}_{\text{out}}^{(i)}$. If the direction of observation, φ, is kept fix and if observations are made for different crystal orientations θ, each of the $\mathbf{k}_{\text{out}}^{(i)}$ vectors will generate a scattering surface $S^{(i)}$. If the scattering surfaces so generated happen to be nearly parallel to the direction of ingoing wave vectors $\mathbf{k}_{\text{in}}^{(i)}$ it is seen that all the scattered wave vectors $\mathbf{k}_{\text{out}}^{(i)}$ very nearly have the same length (case a). We have a focusing effect, which permits us to use for instance the longest $\mathbf{k}_{\text{in}}$ vector corresponding to $\lambda_{\text{in}} = 3.952$ Å to define the energy gain as indicated in figure 2 for the intensity maximum (a). Also it is obvious that this mechanism of formation of an intensity maximum is equivalent to a considerable intensity gain as all the available intensity of the ingoing spectrum is used in the formation of one single peak. On the other hand if the scattering surfaces generated by the different $\mathbf{k}_{\text{in}}^{(i)}$ vectors make a larger angle with the vectors $\mathbf{k}_{\text{in}}^{(i)}$ the vectors $\mathbf{k}_{\text{out}}^{(i)}$ vary in lengths as indicated in figure 3*b*. If now the differential cross section for the scattering process is such that

$$\sigma(\mathbf{k}_{\text{in}}' \to \mathbf{k}_{\text{out}}') \geqslant \sigma(\mathbf{k}_{\text{in}}'' \to \mathbf{k}_{\text{out}}'') \geqslant \sigma(\mathbf{k}_{\text{in}}''' \to \mathbf{k}_{\text{out}}''') \text{ and so on,}$$

---

[1] In figure 3 actually parts of the intersections of the different scattering surfaces with the principal plane under discussion are given.

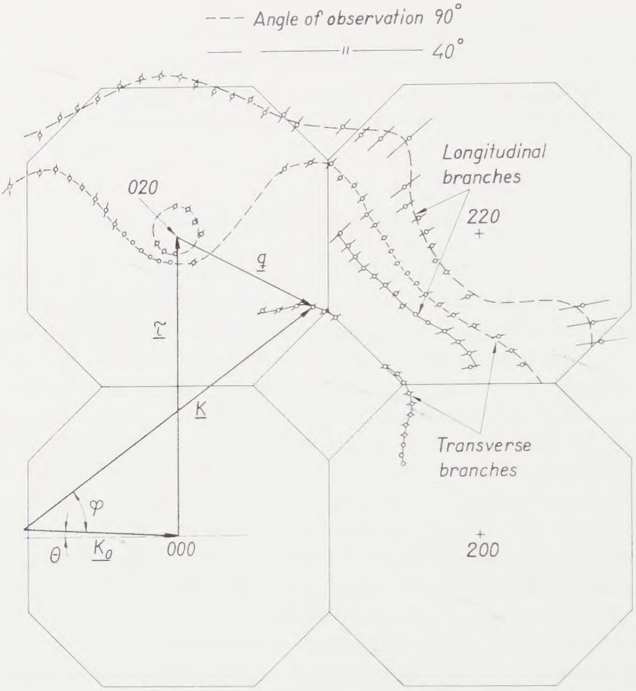

Fig. 4. Experimentally determined scattering surfaces at two different angles of observation and room temperature.

the scattered spectrum will reproduce the form of the ingoing beryllium filtered spectrum as shown. This permits us to use the wave length shift of the beryllium break at 3.952 Å to define the energy gain as indicated in figure 2 for the intensity maximum (b). This discussion may of course be carried on for other possible scattering pictures, and it is found that with the exception of directions near singular directions [11] it is always possible to use the wave length 3.952 Å to define $\mathbf{k}_{\text{in}}$ and associate it with the corresponding scattered wave length defining $\mathbf{k}_{\text{out}}$. To carry such an investigation through parallel to the collection of experimental data, it is necessary to have some idea of the frequency spectrum of the crystal or rather to know the isofrequency surfaces to a first approximation. Fortunately these had been given by theoretical calculations [12] for the case of aluminium partly based on X-ray measurements [13], so these data were used in combination with the known cross section formulas [1,11] to analyze the observed intensity distributions. As described elsewhere (reference 14, the appendix) small corrections amounting to 1–3 % of the observed shifted beryllium cut off positions on the time-of-flight scale had sometimes to be made as an effect of the finite resolution of the instrument.

c. *Collection of data*

Knowing the principle of interpretation of the data the next experimental problem using a *fix* ingoing wave length, 3.952 Å, is to fill the reciprocal lattice plane, 001, with experimentally determined phonon wave vectors $\mathbf{q}$ and corresponding frequencies ω

to be able to construct the dispersion relations $\omega = \omega(\mathbf{q})$. This is, however, possible using the full ability of the experimental equipment. If the angle of observation increases, the momentum transfer in the scattering process, $\mathbf{k}_{\text{out}} - \mathbf{k}_{\text{in}} = \varkappa$, also increases for the vector $\varkappa$ having a fix direction in the reciprocal lattice. This property of the scattering process immediately suggests the method to use:

1. for a fix angle of observation, φ, the crystal orientation is varied in small angular steps—in the actual observation in steps of 2.5°—and the scattering surfaces are determined for this angle of observation.
2. the same series of observations is repeated for different angles of observations, the scattering surfaces being determined for each angle φ.

In practice because of the symmetry properties of the crystal the observations can be limited to a 45° interval in the first Brillouin zone. Most of the observations to be described were made in the zone round the 220 reciprocal lattice point. The reason for this choice was that both the high and low frequency branches here give scattered neutron intensities concentrated into rather narrow peaks because of the focusing effect illustrated in figure 3*a*. Typical results gained at room temperature are illustrated in figure 4. The observations at $\varphi = 90°$ were made over a wide region of angular settings of the crystal to test the ideas outlined above. The observations at $\varphi = 40°$ are typical for the series of measurements made at other angles φ and similar observations were made at $\varphi = 83$, 80, 70, 60, 50 and 30°.

III. Room temperature results ($T = 293°$ K)

In the way described in the preceding section about 400 phonons were determined at room temperature of the crystal, all these phonons falling in the 001 plane. Because of the symmetry of the crystal all of them are moved into a 45° sector of the first Brillouin zone falling between the [100] and [110] directions. With a few exceptions for cases of weak intensity or for cases where the interpretation of the data was more complex, the accuracy of the measurements is such that the q vectors are determined to $\pm(3\text{–}5)\,\%$ and similarly the frequencies ω also are known to an accuracy of $\pm(3\text{–}5)\,\%$ in general. With all the experimentally determined points moved into the 45° sector, lines were drawn from the 220 reciprocal lattice point with 5° intervals, in all 10 directions between [100] and [110] and including those, i.e. [100], [100] + 5°, [100] + 10° ... [110]. All experimental points falling within ±1° from these lines were used to determine points on the 10 dispersion curves. In those cases when the experimentally determined phonon vectors did not fall within ±1° from the selected direction the intersection between the scattering surface and this direction was used to define the phonon on the dispersion curve. This resulted in about 300 phonons being determined and the resulting $\omega(\mathbf{q})$ relations are given in the table of appendix I. Examples of the results for three directions are given in figure 5. For the [100] and [110] directions the results of X-ray measurements [13] are also given for comparison. There seems to be a definite discrepancy for the high frequency, the "longitudinal", branch, the neutron data giving sligtly higher frequencies. For the low energy branch, the "transverse", there is good agreement in the [100] direction and a marked disagreement in the [110] direction, again the neturon data giving higher frequencies.

Although no serious attempt was made to compare the present data to theory—mainly because it was felt that the fitting of trial models has little value until a new

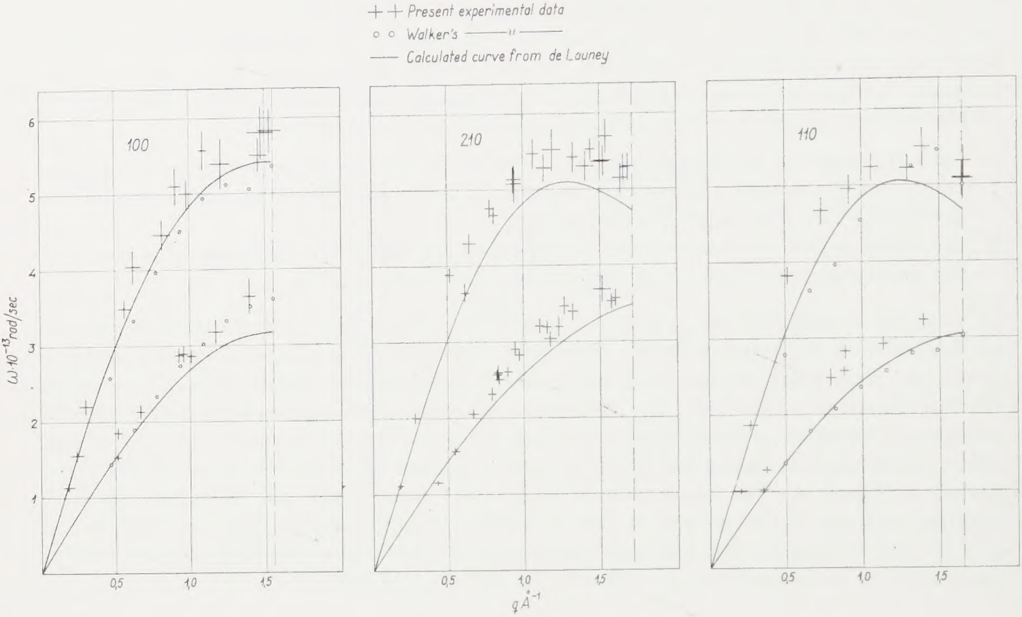

Fig. 5. Dispersion curves determined in the present experiment compared to X-ray and theoretical data.

fundamental treatment of the dynamical problem is made—a simple model was used to calculate the dispersion curves in the directions for which experimental dispersion relations had been found. The model used in this calculation[1] was that due to de Launey [15]. In this model central forces are supposed to act between an atom and its nearest neighbours corresponding to one force constant and between the atom and its next nearest neighbours corresponding to a second force constant. Furthermore the effect of the electron gas surrounding the ions is taken into account in such a way that the "impure" high, medium and low frequency vibration vectors are divided up into three new "pure" vectors of which one is longitudinal and two are transverse. The electron gas is supposed to resist compression, i.e. to affect the pure longitudinal components of the waves but not the transverse components. A correction to the forces is thus introduced using the electron gas bulk modulus. The dynamical problem is completely determined by the three elastic constants c_{11}, c_{12} and c_{44}. Even if the physical meaning of such a model did not seem quite clear, for our purposes such a model appeared to have certain advantages as the variation of the frequencies with temperature could be determined from the known temperature dependence of the elastic constants [16] in a first approximation. The results of these calculations are shown as solid curves in figure 5. The values of the elastic constants at 293°K were used. Although there is no good quantitative agreement between theory and experiment the tendency of this relatively simple theory is in amazingly good agreement with experiment.

---

[1] Carried out by Dr. Alf Sjölander, now at Argonne National Laboratory, U.S.A.

IV. Results gained at elevated temperatures $293 < T \leqslant 932°$ K

a. *Experimental technique*

In making neutron scattering experiments at elevated temperatures one is confronted with the problem of constructing a reliable heating system capable to maintain the crystal at a high constant temperature without gradients and yet this oven should not scatter or absorb neutrons to any appreciable extent. In a first version, for use in the temperature range $300 \leqslant T \leqslant 800°$K, a thin mica sheet, ~ 0.5 mm thick, was wrapped round the crystal as insulator and then a flat resistance band was wired directly on the mica. The crystal with this simple direct heating system was placed in a polished, larger steel container of 0.5 mm wall thickness closed on all sides to secure a certain degree of heat insulation from the surroundings. The temperature was controlled by three thermocouples penetrating to different depths into the crystal. The crystal was mounted between two pins in such a way that it could be rotated round its [001] direction.

In a later version when the crystal was heated up to the melting point a thin steel container was made fitting exactly over the crystal to hold and contain it and again the same technique was used to insulate and heat it. The thermocouples used to measure and control the temperature by automatic regulation of the heating current ensured a temperature definition to $\pm 5°$K all over the crystal volume.

Even if great care was taken to make the oven thin relative to neutron scattering, some background scattering was observed particularly for the highest temperatures. Therefore separate background runs with an empty oven system were made for each temperature used and for different angles of observation as the most important background caused by the oven was the inelastic scattering from iron in it. This background never exceeded 15–20 % of the measured effect from the aluminium crystal.

b. *Results*

As it could be expected the multi-phonon—particularly two-phonon—scattering events should get an increasing importance at higher crystal temperatures, it was necessary to make a careful choice of the position in the reciprocal lattice where one should try to study the one-phonon process. In accordance with the discussion given in section II*b*, it would be of great advantage if the intensity of the ingoing spectrum could be concentrated into one *narrow* intensity maximum in the one-phonon scattering process as illustrated in figure 3*a*. Fortunately this happens for the longitudinal as well as for the transverse branches in a region of the reciprocal lattice near the 220 reciprocal lattice point. Therefore a first series of runs was made at an angle of observation of $\varphi = 90°$ and a crystal orientation defined by the angle $\theta \sim 65°$ and first for crystal temperatures in the range $293 \leqslant T \leqslant 793°$K. The results of these first measurements are given in figure 6. In this figure are also given results of a later run at $T = 910°$K and a final run taken at the melting point a 932°K. From this first series of runs two effects were clearly observed and the possibility of a third effect appeared:

1. A multi-phonon spectrum rapidly grows up for increasing temperature and becomes dominant at about 700°K.
2. The one-phonon lines shift their position in such a way that the frequency ω, defined by the neutron energy gain, decreases with temperature.

3. Also the one-phonon lines seemed to broaden. At least this effect was observed at the highest temperatures. This effect was, however, difficult to estimate from this first run because of the strong multi-phonon scattering.

From these first observations it was thus obvious that the change of the dispersion curves $\omega = \omega(\mathbf{q})$ with temperature could be measured, if the direction of observations was chosen in the proper way. Also the multiphonon spectrum as well as the line width could be studied, if one could find a position in the reciprocal lattice where the scattered neutron intensity caused by the "longitudinal" phonon was zero. If furthermore the frequency of the phonon studied could be chosen relatively low this would mean that the multi-phonon spectrum and the one-phonon line would be separated from each other on the wave length or time-of-flight scale. Actually it was possible to find such a place in the reciprocal lattice choosing a direction of observation of $\varphi = 50°$ and a crystal orientation defined by $\theta \sim 60°$. As the phonon line widths and line shifts are intimately connected to the question of anharmonicity of the forces acting between atoms, we went into a detailed study of the temperature effects. The observation of the three phenomena will now be treated separately.

1. *Variation of frequencies ω with temperature*

Knowing the dispersion relations at room temperature and with the information from the first runs at higher temperatures (figure 6) it was possible to choose such combinations of angles of observations, φ, and crystal orientations, θ, that for each temperature the phonons could be determined along *one* direction in the reciprocal lattice, i.e. the dispersion curve could be determined directly for each temperature investigated. The direction selected was one making an angle of $\sim 18°$ with the [100] direction in the 001 plane corresponding to the [310] direction. The phonon wave vectors determined in this way always fell within $\pm 2°$ from the desired direction. Thus the dispersion relations were determined for this direction for temperatures 293, 387, 486, 700 and 793°K for the high frequency branch and for 293 and 793°K for the low frequency branch. Figure 7 shows these dispersion curves as well as the ones calculated using the model of the Launey. The temperature variation of the theoretical curves was derived from the measured temperature dependence of the elastic constants [16]. In calculating the experimental curves from the measured scattered neutron spectra due consideration was given to the volume expansion of the crystal (contraction of the reciprocal lattice). In determining the position on the time-of-flight scale of the one-phonon peaks, it was carefully studied, if this position could be affected by the multi-phonon spectrum on which the peaks were superimposed (compare figure 6). The true shape of the multi-phonon spectrum could be calculated to good accuracy using the theory of Sjölander (compare following sections).

Again it is striking how the simple model of de Launey predicts a variation of frequency which gives the general tendency reasonably well. Quantitatively there is no agreement as the predicted temperature variation for a fixed $q/q_{\max}$ is about 50 % higher than the measured.

To investigate how the frequency varies with temperature for a constant $q/q_{\max}$, the frequency values read from the experimental dispersion curves drawn in figure 7 for different constant values of $q/q_{\max}$ were plotted against temperature. The result is given in figure 8 where also are added the result of some studies at higher tempera-

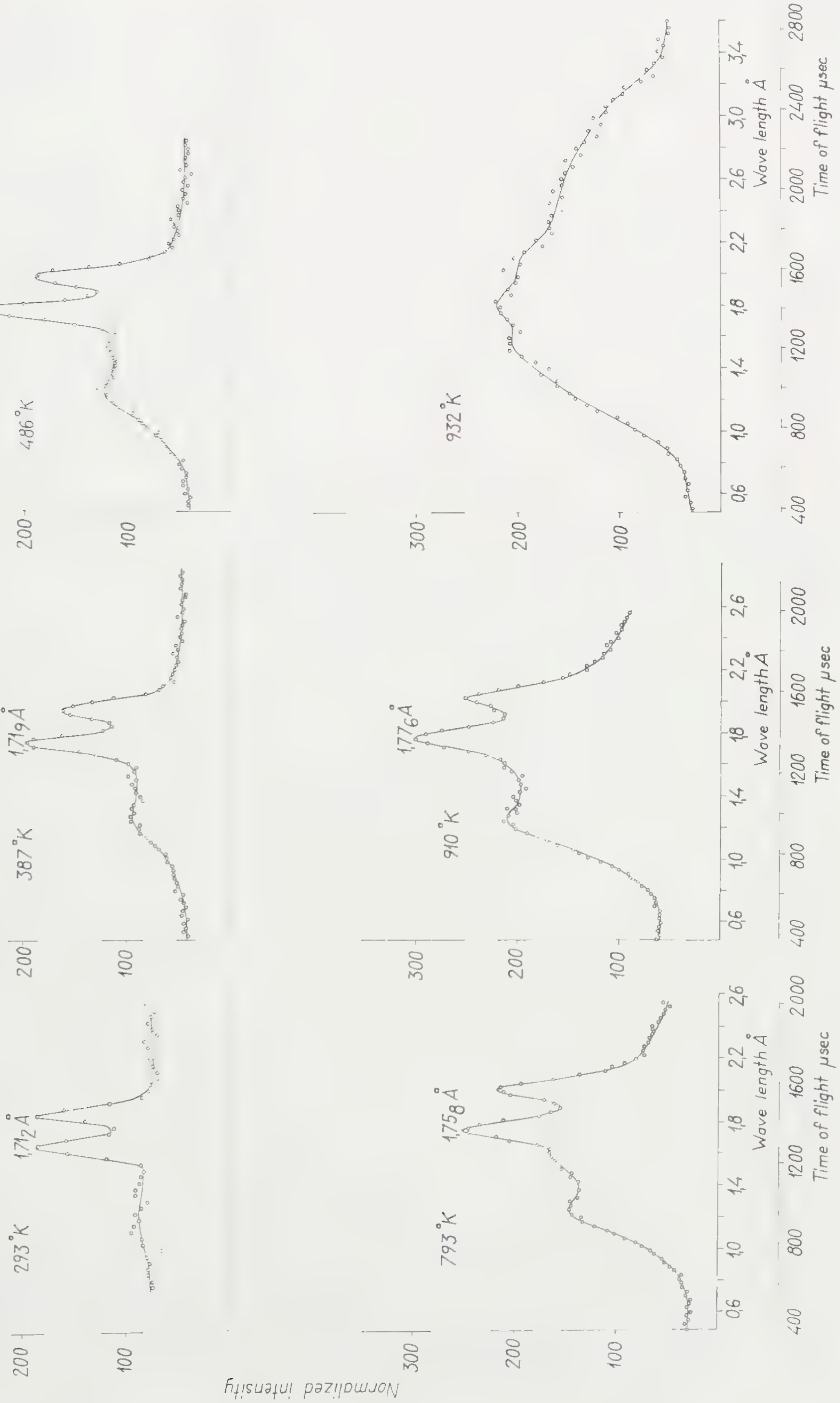

Fig. 6. Scattered spectra observed at different temperatures.

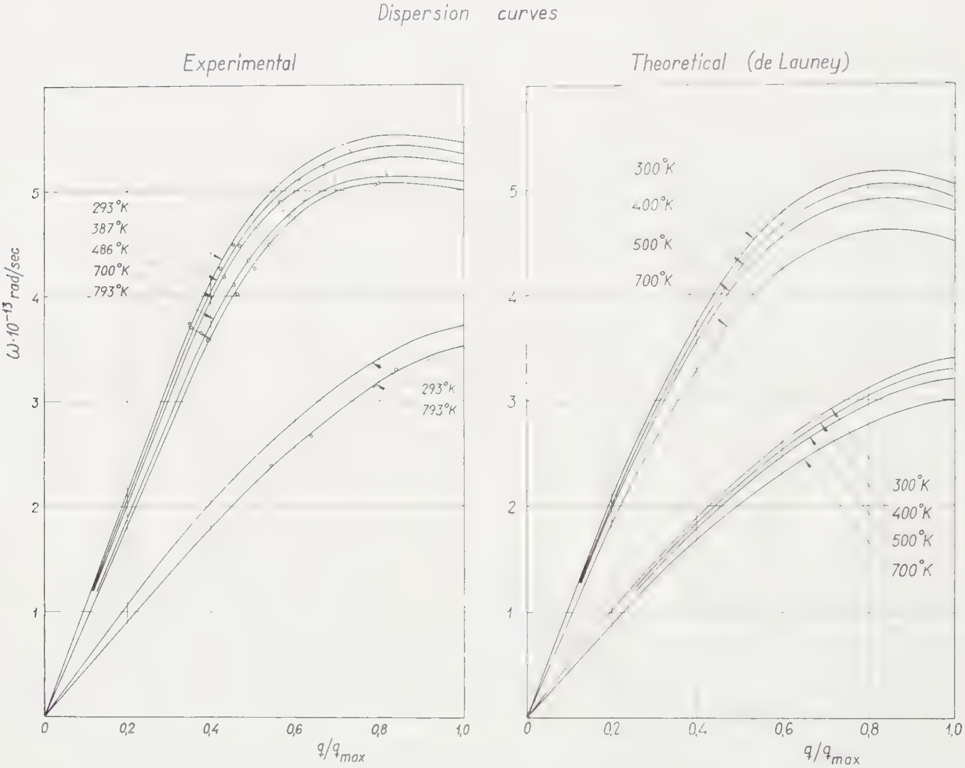

Fig. 7. Experimentally determined dispersion curves in the direction [310] at higher temperatures (left) compared to the theoretical ones (right).

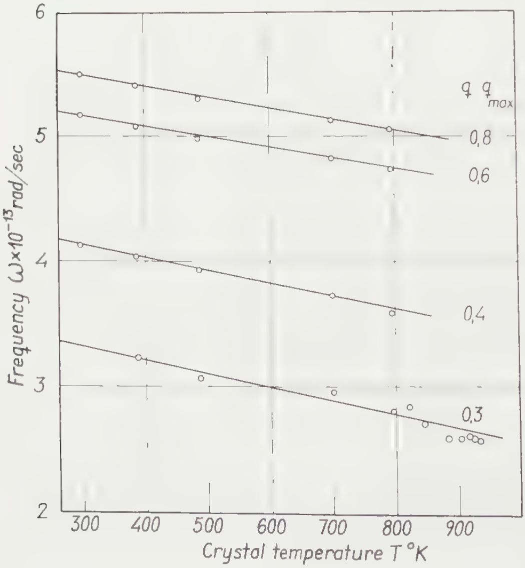

Fig. 8. Variation of frequencies with temperature for the high frequency branch, each curve corresponding to a constant ratio $q/q_{\max}$.

tures for $q/q_{\max} = 0.3$. The frequencies vary linearly with temperature even up to the highest temperatures near the melting point. Also the slope of the lines is independent of the value of $q/q_{\max}$ in the region. $0.3 < q/q_{\max} < 0.8$, we have investigated. The frequency variation with temperature is well described by the formula

$$\omega(\mathbf{q}, T) = \omega(\mathbf{q}, T_0) - (9.5 \pm 1.0) \cdot 10^9 (T - T_0) \tag{2}$$

So far this temperature variation of the frequencies is thus studied for one direction in the 001 plane of the reciprocal lattice. To attempt to estimate the agreement or disagreement of these results with the measured temperature variation of the Debye temperature, θ_D, of aluminium, let us assume that the frequencies for any direction in the crystal vary in the same way. If we take a frequency of about $4 \cdot 10^{13}$ rad/sec as an average frequency in the spectrum, we find the percentage variation of this frequency to be about 12 % in going from 300°K to 800°K. According to X-ray measurements of Owen and Williams [17] the Debye temperature varies about 15 % over the same temperature range. The present neutron results thus do not seem to contradict X-ray results.

2. *Variation of line width with temperature*

To be able to study the line width variation it was necessary to find a low frequency phonon, which in the scattering process should produce an intensity maximum as narrow as possible and as well separated from the multi-phonon spectrum as possible. As mentioned earlier in this section it was possible to find such a combination of angles φ and θ that these conditions were reasonably well fulfilled. Figure 9 shows the scattering pictures obtained for $\varphi = 50°$ and $\theta = 60°$ and for the temperatures 293, 486, 700, 854 and 923°K. All backgrounds are subtracted. Similar observations were made at a large number of temperatures between 773 and 932°K. A striking effect is that the definition of the one-phonon lines persists even up to the immediate neighbourhood of the melting point. The multi-phonon spectrum is reasonably well separated from the single one-phonon maximum, such that the multi-phonon part may be subtracted from the intensity under the one-phonon peak as indicated in the figure by the dotted lines at the base of the one-phonon peaks. To perform this subtraction the theoretical multi-phonon spectra discussed in the next section were of great assistance. After this subtraction the widhts of the one-phonon line were analyzed in the following way:

The line width observed is built up of three different contributions: a. the width of the line caused by the wave length spread in the ingoing spectrum $\delta\lambda_i$ (compare figure 3*b*),[1] b. the resolution width, $\delta\lambda_r$, which was 90 μs or 0.116 Å, c. the natural line width $\delta\lambda_n$, which we want to determine. As there are three factors which make up the total, observed line width $\delta\lambda_0$, it is a reasonable approximation to use the formula

$$\delta\lambda_n = \sqrt{\delta\lambda_0^2 - \delta\lambda_i^2 - \delta\lambda_r^2} \tag{3}$$

to calculate $\delta\lambda_n$, i.e. to assume the components to have approximately Gaussian shape. For temperatures below 600°K the line width $\delta\lambda_n$ obviously was so small, that it could not be observed, i.e. $\delta\lambda_0 = \sqrt{\delta\lambda_i^2 + \delta\lambda_r^2}$. Of the two contributions to $\delta\lambda_0$, the resolution width, $\delta\lambda_r$, certainly stays constant. It remains, however, to show that

---

[1] Actually the "one" phonon peak is not just formed by one single phonon but by a band of phonons corresponding to a 15–20 % spread, from $\frac{q}{q_{\max}} \sim 0.55$ to $\frac{q}{q_{\max}} \sim 0.65$.

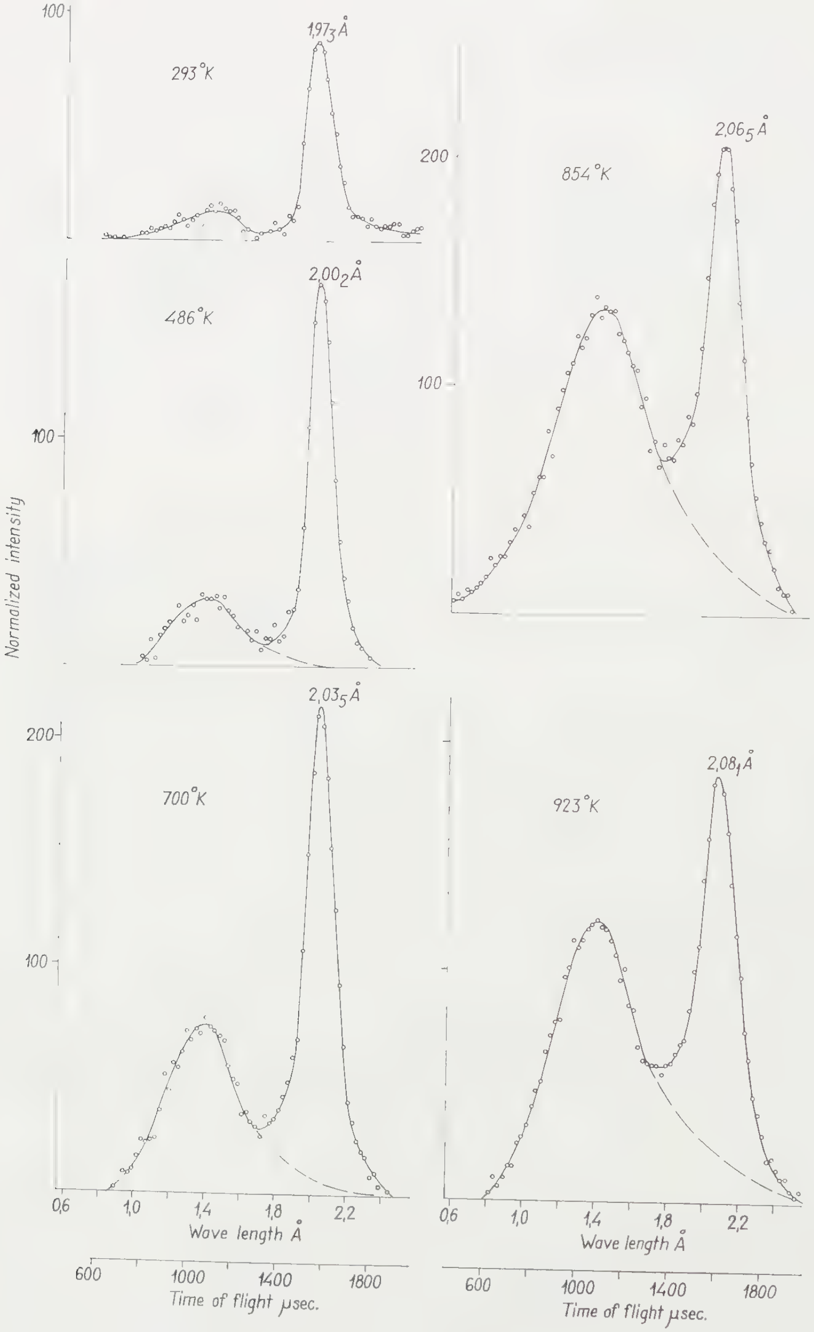

Fig. 9. Types of observed scattered spectra used to analyze line widths.

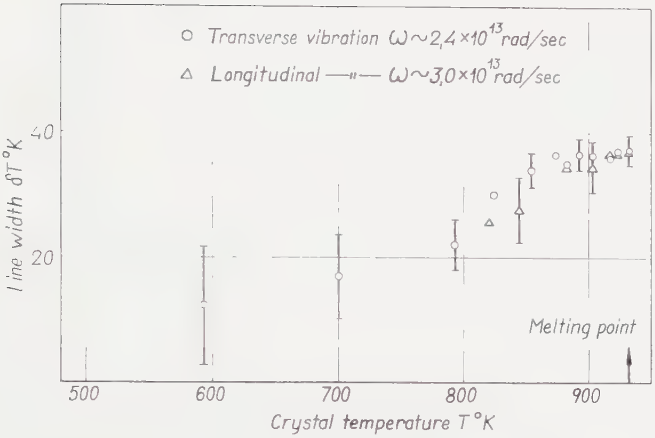

Fig. 10. Phonon line width as a function of temperature.

$\delta\lambda_i$ also stays constant, such that any observed increase in width really is caused by an increase in the natural line width, $\delta\lambda_n$. A variation of $\delta\lambda_i$ should mean that the angle between the vectors $\mathbf{k}_{\text{out}}^{(i)}$ and the scattering surfaces $S^{(i)}$ should change with temperature (see figure 3*a* or *b*). By differentation of the energy and momentum relations (1) and using the measured dispersion curves it is, however, possible to show that the change in the line width caused by this effect certainly is less than 4°K over the temperature range of our measurements. As already mentioned, for temperatures below 600°K the width of the line stayed constant and equal to 135 μs or 0.174 Å. The accuracy to which this could be determined was about ± 5 μs. From 600°K and on a monotonous increase could be observed ending up with a width of about 180 μs or 0.232 Å near the melting point. The analyzed results with the phonon line width expressed in °K are given in figure 10 and appendix II. Included are also a few results, which could be gained by analyzing in the same way the width of a "longitudinal" phonon of similar frequency.

In order to estimate the mean life time and the mean free path of the phonons studied, a calculation of the line shape assuming an exponential damping was carried out.[1] Assuming the phonon waves described by

$$\mathbf{u}_{\mathbf{R}} = \mathbf{c}\, e^{i(\mathbf{q}\cdot\mathbf{R}-\omega_s t)} \cdot e^{-\gamma_s|t|} \tag{4}$$

and working the differential scattering cross section out using this assumption, it turns out that the cross section instead of δ-functions of the form $\delta(\omega-\omega_0-\epsilon\,\omega_s)$ for the case $\gamma_s = 0$ will now contain a factor describing the line shape

$$F_s(\omega-\omega_0-\epsilon\,\omega_s) = \frac{1}{\pi\gamma_s}\cdot\frac{1}{1+\left(\dfrac{\omega-\omega_0-\epsilon\,\omega_s}{\gamma_s}\right)^2}, \tag{5}$$

where $\hbar(\omega-\omega_0)$ is the neutron energy gain ($\epsilon = \pm 1$), $\hbar\,\omega_s$ is the energy of the phonon. This result may be interpreted in the way that when damping is present the energy

---

[1] The calculation carried out by Dr. Alf Sjölander.

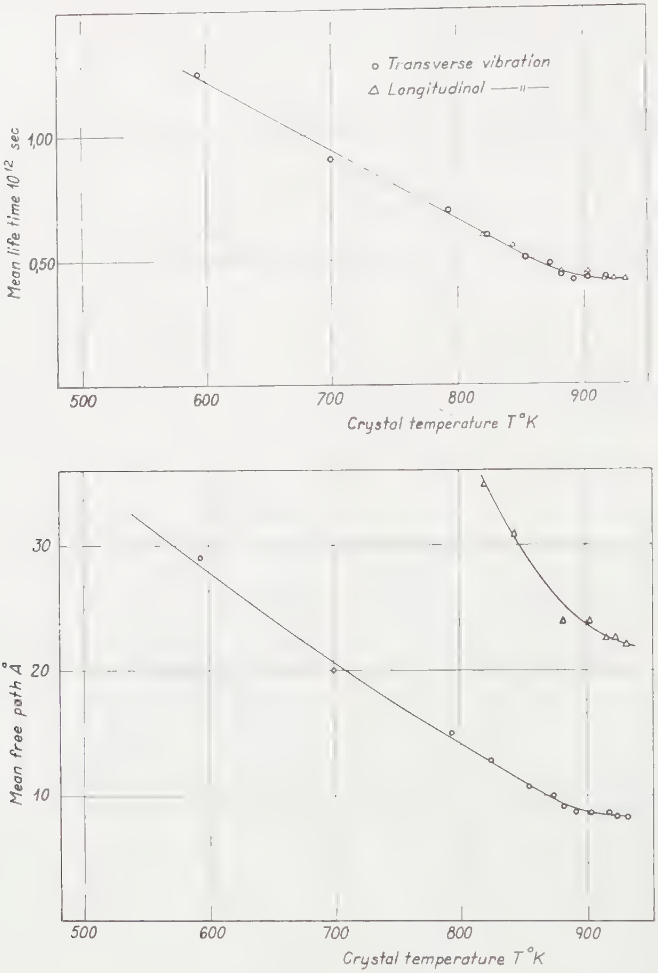

Fig. 11. Phonon mean life time and mean free path as a function of temperature.

conservation law is not strictly fulfilled. The line gets a width corresponding to energy exchange between phonons during the damping. It is thus obvious that the full width, ΔE, at half maximum for this line shape is $2\gamma_s \cdot \hbar$. The mean life time, Δt, is from eq. (4) $1/\gamma_s$ such that $\Delta E \Delta t = 2\hbar$. Using the measured line widths, δT°K, it is then easy to calculate the mean life time $\Delta t = 2\hbar/k_B\delta T$, where k_B is the Boltzmann constant. Knowing the mean life time, this is multiplied by the wave velocity to get mean free path. Because the phonons studied are both to be found on the almost linear portion of the dispersion curves—$q/q_{\max} \sim 0.6$ for the "transverse" phonon with $\omega \sim 2.4 \cdot 10^{13}$ rad/sec and $q/q_{\max} \sim 0.3$ for the "longitudinal" phonon with $\omega \sim 3.0 \cdot 10^{13}$ rad/sec—it is immaterial if the phase or group velocity is used to calculate the mean free path. The mean life times and mean free paths thus derived are given in figure 11. As the wave lengths of the transverse and longitudinal phonons studied are about 6 Å and

14 Å respectively, these observations indicate that the mean free paths vary from about 5 times the phonon wave length at 600 K to about 1.5 times the phonon wave length near the melting point. The damping of the phonon waves is thus very strong, indicating the harmonic approximation to be rather doubtful at these crystal temperatures.

3. *The multi-phonon spectrum*

As already illustrated best by figure 9 the multi-phonon spectrum rapidly grows up when the crystal temperature exceeds the Debye temperature of the crystal. A calculation of this spectrum for the coherent scattering case is of almost prohibitive complexity. The cross section has, however, been given in convenient form in the incoherent approximation. Sjölander [5] has given the differential cross section in the form of a phonon expansion (see ref. 5, formulas II.28 and II.29), which is just a form suitable for comparison with the present experiment.

However, before the data may be compared to theory all backgrounds have to be carefully subtracted. In measuring a continuous, broad spectrum of this type using a crystal of large dimensions the problem of multiple scattering is of greatest importance. Therefore this phenomenon was studied at length both experimentally and theoretically. As indicated by calculations the multiply scattered neutron spectra should be of a shape similar to the multi-phonon spectrum giving proportionally greater contributions to the observed spectrum for smaller neutron energy gains. To investigate the multiple effect experimentally several different experiments were tried. In one case an aluminium poly-crystal of the same size as the single crystal was cut into two halves along its cylinder axis. At temperatures of 600°K and 800°K first an upper half was irradiated by the now well collimated beam, this beam only seeing this upper half and the scattered spectrum was recorded at angles of observation of $\varphi = 90°$ and $50°$. Then the lower half was added but not irradiated directly and the scattered spectra were again recorded. When the spectra thus recorded were compared for constant φ, they were found to coincide within the statistical accuracy of about 3–4 %, so there was no observable change in intensity or spectrum shape caused by multiply scattered neutrons from the lower half. Then the same sort of experiment was repeated now reversed, i.e. with the lower half irradiated and the two different kinds of spectra were recorded. When compared they were again found to have the same shape within ±4 % but the intensity for the case when both halves were present was found to have decreased by about 10 %. This decrease is, however, what can be expected from the thickness and cross section, if the upper half in this case merely acts as an absorber and outscatterer for neutrons coming from the lower half. Thus there was no observable effect due to multiple scattering.

In another experiment we irradiated again at 600°K and 800°K firstly a solid aluminium poly-crystal of cylinder shape and secondly an aluminium tube of the same diameter, 6 cm, as the solid cylinder. As the tube wall thickness was 0.6 cm in the case of the hollow cylinder, the multiple scattering effect should be much smaller than in the case of the solid cylinder. Again, however, the two scattered spectra as compared for constant angle of observation were of the same shape within the statistical accuracy.

From all these negative results we could only draw the conclusions that either the multiple scattering is small or that the multiply scattered spectrum should have the same shape as the single scattered spectrum. Consequently we could not apply any corrections for the multiple scattering to the observed multi-phonon spectrum.

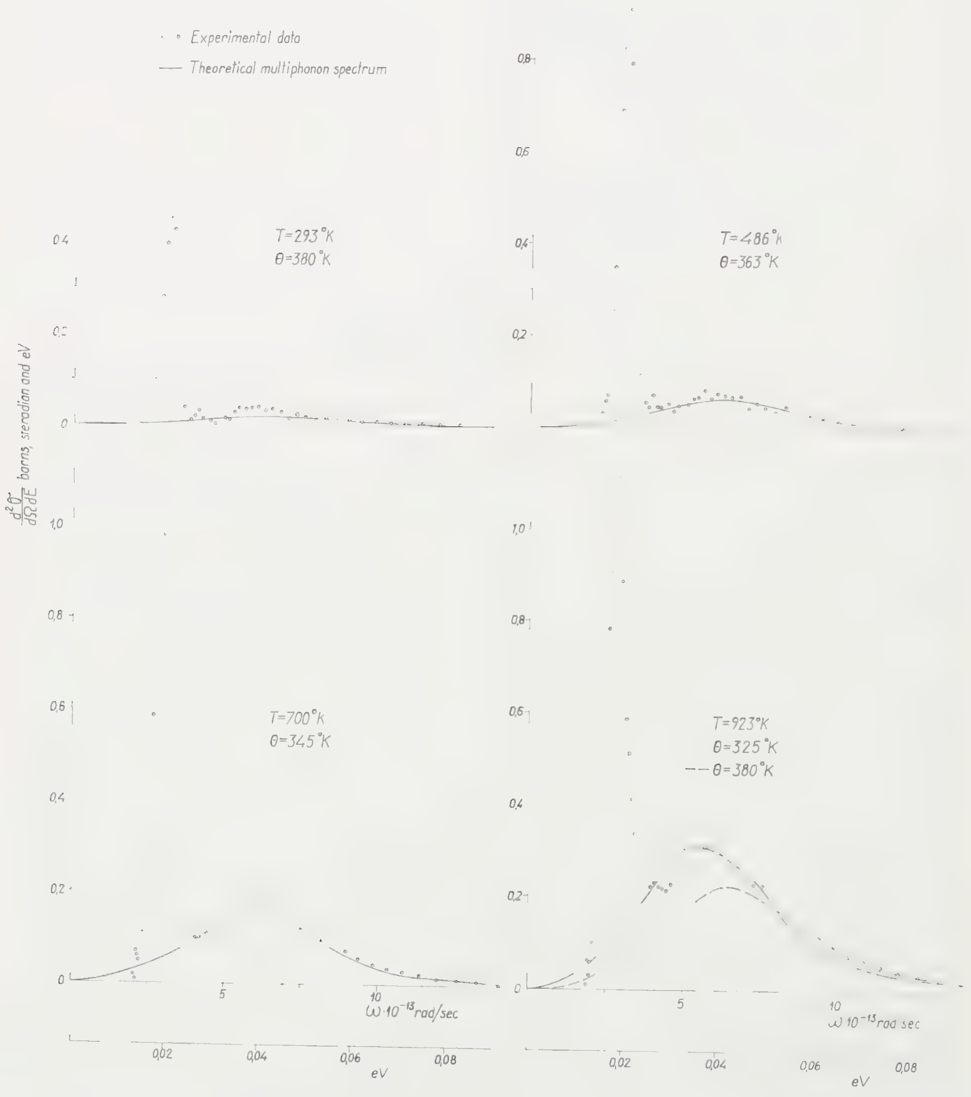

Fig. 12. Observed multi-phonon differential cross sections compared to the theoretical ones.

After these negative results we undertook to measure the differential cross section absolutely. To perform this the flux hitting the sample crystal was measured absolutely, the effective solid angle of observation was carefully analyzed and calculated, the true chopper transmission was measured absolutely, and the measured intensities were corrected for the air scattering in the flight path and for the finite detector thickness. Even with the greatest care in all calculations and measurements the final uncertainty, however, is about 25 %. The cross sections were also calculated absolutely for different crystal temperatures using Sjölander's formulas. As the Debye temperature, θ_D, enters critically into these calculations a linear variation of θ_D from $\theta_D = 380$°K at $T = 293$°K to $\theta_D = 325$°K at $T = 923$°K was assumed. This amounted to a 14 % variation of θ_D over this temperature range, a reasonable variation in the light of these measurements and of the measurements of Owen and Williams. For comparison a calculation of the cross section at $T = 923$°K was also made assuming θ_D constant $= 380$°K. In calculating the cross section at the highest temperatures up to five-phonon processes were included. Also the cross section was integrated over the ingoing spectrum shape to be comparable with experimental data. Finally the experimental resolution function was applied to the theoretical curves. The result of these calculations are given in figure 12 as well as the experimental points. The experimental values are normalized to the theoretical at $T = 923$°K as there was some disagreement (although it happened to be small) between the absolutely calculated and measured values. The cross section is given on an absolute energy (ω) scale such that the ingoing spectrum is to be found below $\omega \sim 0.8 \cdot 10^{13}$ rad/sec. As seen from this figure there is a rather satisfactory agreement between theory and measurement. The fact that the incoherent approximation so well describes the cross section indicates that the coherence effects in two- and certainly in higher-phonon processes are averaged out in these multi-phonon scattering events. Also the curve shown for the case of 923°K and $\theta_D = 380$°K shows that the variation of θ_D with temperature certainly has to be taken into account to explain the variation of the inelastic scattering cross section with temperature, a fact already found for total cross section measurements [18].

ACKNOWLEDGEMENT

During the measurements we have had many stimulating discussions with Dr. Alf Sjölander. These discussions have been of greatest importance for us as well as the calculations carried out by him.

REFERENCES

1. I. Waller and P. O. Fröman, Ark. Fys. *4*, 183 and 191 (1952).
2. G. Placzek and L. van Hove, Phys. Rev. *93*, 1207 (1954).
3. R. S. Carter, H. Palevsky and D. J. Hughes, Phys. Rev. *106*, 1168 (1957).
   B. N. Brockhouse and A. T. Stewart, Rev. Mod. Phys. *30*, 236 (1958).
4. A. T. Stewart and B. N. Brockhouse, Rev. Mod. Phys. *30*, 250 (1958).
   C. M. Eisenhower, I. Pelah, D. J. Hughes and H. Palevsky, Phys. Rev. *109*, 1046 (1958).
5. Alf Sjölander, Ark. Fys. *14*, 315 (1958).
6. Alf Sjölander, Ark. Fys. *13*, 215 (1958).
7. K. E. Larsson, R. Stedman, and H. Palevsky, J. Nuclear Energy *6*, 222 (1958).
8. I. Pelah, C. M. Eisenhower, D. J. Hughes and H. Palevsky, Bull. Am. Phys. Soc. Ser. II, *2*, 43 (1957).
9. K. E. Larsson, U. Dahlborg, S. Holmryd, K. Otnes and R. Stedman, Ark. Fys. *16*, 199 (1959).
10. H. Palevsky, K. Otnes and K. E. Larsson, Phys. Rev. *112*, 11 (1958).
11. Alf Sjölander, Ark. Fys. *13*, 199 (1958).
12. G. L. Squires, Phys. Rev. *103*, 304 (1956).
13. C. B. Walker, Phys. Rev. *103*, 547 (1956).
14. K. E. Larsson and K. Otnes, Ark. Fys. *15*, 49 (1959).
15. Jules de Launey, J. Chem. Phys. *21*, 1975 (1953).
16. Paul M. Sutton, Phys. Rev. *91*, 816 (1953).
17. E. A. Owen and R. W. Williams, Proc. Roy. Soc. (London) *A 188*, 509 (1947).
18. L. S. Kothari and K. S. Singwi, Phil. Mag. *2*, 694 (1957).

APPENDIX I

Frequencies for given phonon wave vectors.

Direction in the 001-plane. ($\alpha = 0° = [100]$-direction, $\alpha = 45° = [110]$-direction)	Longitudinal		Transverse	
	$q/q_{\max}$	$\omega \times 10^{-13}$ rad/sec	$q/q_{\max}$	$\omega \times 10^{-13}$ rad/sec
0° $q_{\max} = 1.551$ Å^{-1}	0.120±0.024	1.13±0.05	0.330±0.017	1.53±0.04
	0.160±0.030	1.55±0.07	0.333±0.017	1.85±0.05
	0.200±0.031	2.20±0.10	0.432±0.017	2.13±0.09
	0.361±0.026	3.49±0.12	0.598±0.017	2.87±0.10
	0.400±0.030	4.05±0.22	0.617±0.017	2.89±0.11
	0.532±0.037	4.47±0.20	0.650±0.017	2.86±0.08
	0.583±0.025	5.11±0.25	0.751±0.031	3.18±0.16
	0.632±0.030	5.01±0.18	0.900±0.050	3.65±0.23
	0.703±0.017	5.58±0.26		
	0.780±0.047	5.40±0.33		
	0.940±0.037	5.51±0.22		
	0.950±0.058	5.81±0.35		
	0.988±0.050	5.84±0.29		
5° $q_{\max} = 1.557$ Å^{-1}	0.393±0.036	4.02±0.18	0.303±0.017	1.77±0.05
	0.423±0.036	4.15±0.22	0.318±0.017	1.46±0.04
	0.491±0.036	4.39±0.19	0.352±0.017	1.63±0.06
	0.552±0.017	5.02±0.17	0.395±0.017	2.00±0.07
	0.574±0.036	4.56±0.23	0.461±0.017	2.28±0.08
	0.602±0.030	4.87±0.17	0.561±0.017	2.69±0.09
	0.660±0.033	5.22±0.25	0.600±0.017	2.79±0.10
	0.667±0.017	5.44±0.22	0.630±0.017	2.77±0.09
	0.746±0.017	5.76±0.35	0.683±0.025	3.04±0.12
	0.755±0.041	5.27±0.25	0.697±0.017	3.22±0.10
	0.801±0.020	5.86±0.29	0.720±0.033	3.10±0.13
	0.866±0.050	5.67±0.33	0.859±0.036	3.48±0.17
	0.929±0.036	5.53±0.22	0.968±0.017	3.73±0.14
	0.932±0.050	5.74±0.26	0.990±0.036	3.75±0.21
	0.965±0.036	5.50±0.22	1.000±0.033	3.77±0.21
	0.997±0.017	5.93±0.25		
	1.000±0.045	5.80±0.27		
	1.000±0.050	5.81±0.27		
10° $q_{\max} = 1.576$ Å^{-1}	0.362±0.025	3.95±0.12	0.182±0.016	0.93±0.03
	0.456±0.033	4.20±0.24	0.282±0.016	1.70±0.05
	0.462±0.029	4.34±0.14	0.298±0.016	1.38±0.03
	0.521±0.016	5.01±0.17	0.364±0.016	1.75±0.05
	0.579±0.020	4.74±0.11	0.367±0.016	1.87±0.05
	0.638±0.016	5.36±0.20	0.487±0.016	2.45±0.10
	0.675±0.016	5.33±0.21	0.507±0.016	2.46±0.10
	0.677±0.031	5.25±0.21	0.570±0.016	2.69±0.10
	0.734±0.020	5.78±0.28	0.590±0.016	2.64±0.06
	0.823±0.049	5.50±0.28	0.682±0.021	3.02±0.10
	0.908±0.045	5.59±0.27	0.716±0.020	3.10±0.13
	0.931±0.029	5.78±0.28	0.721±0.016	3.27±0.11
	0.934±0.038	5.57±0.21	0.787±0.016	3.34±0.11
	0.949±0.057	5.83±0.35	0.823±0.026	3.28±0.13
	0.980±0.049	5.70±0.27	0.928±0.016	3.73±0.09
	0.984±0.044	5.72±0.27	0.984±0.016	3.53±0.12

Appendix I *(cont.)*

Direction in the 001-plane. ($\alpha = 0° = [100]$-direction, $\alpha = 45° = [110]$-direction)	Longitudinal		Transverse	
	$q/q_{\max}$	$\omega \times 10^{-13}$ rad/sec	$q/q_{\max}$	$\omega \times 10^{-13}$ rad/sec
15° $q_{\max} = 1.606$ Å^{-1}	0.346 ± 0.027	3.93 ± 0.13	0.182 ± 0.016	0.93 ± 0.03
	0.438 ± 0.016	4.29 ± 0.15	0.269 ± 0.016	1.61 ± 0.04
	0.499 ± 0.016	4.87 ± 0.17	0.287 ± 0.016	1.28 ± 0.04
	0.551 ± 0.021	4.74 ± 0.11	0.351 ± 0.016	1.75 ± 0.05
	0.604 ± 0.035	5.22 ± 0.31	0.451 ± 0.016	2.34 ± 0.10
	0.609 ± 0.032	5.22 ± 0.19	0.548 ± 0.016	2.66 ± 0.11
	0.688 ± 0.029	5.69 ± 0.31	0.560 ± 0,016	2.65 ± 0.06
	0.765 ± 0.016	5.42 ± 0.21	0.567 ± 0.016	2.72 ± 0.15
	0.778 ± 0.029	5.33 ± 0.27	0.618 ± 0.026	2.91 ± 0.16
	0.881 ± 0.027	5.61 ± 0.28	0.631 ± 0.016	3.01 ± 0.08
	0.881 ± 0.040	5.50 ± 0.20	0.651 ± 0.016	2.95 ± 0.07
	0.937 ± 0.048	5.81 ± 0.35	0.752 ± 0.016	3.31 ± 0.12
	0.939 ± 0.040	5.57 ± 0.22	0.778 ± 0.024	3.16 ± 0.13
	0.945 ± 0.042	5.61 ± 0.26	0.836 ± 0.016	3.73 ± 0.08
	0.948 ± 0.035	5.59 ± 0.21	0.915 ± 0.029	3.48 ± 0.14
20° $q_{\max} = 1.651$ Å^{-1}	0.330 ± 0.019	3.89 ± 0.09	0.183 ± 0.016	0.94 ± 0.03
	0.406 ± 0.028	4.29 ± 0.14	0.333 ± 0.016	1.64 ± 0.05
	0.477 ± 0.016	4.79 ± 0.13	0.416 ± 0.016	2.05 ± 0.08
	0.500 ± 0.019	4.69 ± 0.11	0.433 ± 0.016	2.19 ± 0.09
	0.577 ± 0.028	5.16 ± 0.25	0.483 ± 0.016	2.56 ± 0.10
	0.580 ± 0.031	5.14 ± 0.17	0.530 ± 0.016	2.55 ± 0.06
	0.648 ± 0.031	5.62 ± 0.34	0.548 ± 0.019	2.76 ± 0.14
	0.719 ± 0.028	5.35 ± 0.20	0.575 ± 0.016	2.79 ± 0.07
	0.828 ± 0.016	5.49 ± 0.13	0.608 ± 0.016	2.87 ± 0.07
	0.852 ± 0.043	5.42 ± 0.20	0.727 ± 0.023	3.10 ± 0.10
	0.919 ± 0.034	5.48 ± 0.20	0.730 ± 0.016	3.28 ± 0.11
	0.920 ± 0.047	5.72 ± 0.31	0.766 ± 0.016	3.65 ± 0.08
	0.952 ± 0.019	5.50 ± 0.22	0.781 ± 0.016	3.47 ± 0.14
	0.969 ± 0.038	5.43 ± 0.21	0.838 ± 0.028	3.44 ± 0.12
	0.983 ± 0.025	5.23 ± 0.19	0.866 ± 0.023	3.42 ± 0.09
			0.908 ± 0.016	3.80 ± 0.11
			0.942 ± 0.023	3.77 ± 0.21
			0.969 ± 0.016	3.56 ± 0.13
			1.000 ± 0.023	3.61 ± 0.13
25° $q_{\max} = 1.712$ Å^{-1}	0.108 ± 0.012	1.12 ± 0.05	0.251 ± 0.015	1.16 ± 0.03
	0.168 ± 0.020	2.01 ± 0.07	0.319 ± 0.015	1.57 ± 0.05
	0.303 ± 0.018	3.89 ± 0.09	0.389 ± 0.015	2.06 ± 0.06
	0.359 ± 0.015	3.65 ± 0.12	0.461 ± 0.015	2.32 ± 0.09
	0.377 ± 0.026	4.30 ± 0.13	0.481 ± 0.015	2.57 ± 0.07
	0.455 ± 0.015	4.76 ± 0.12	0.484 ± 0.015	2.60 ± 0.10
	0.469 ± 0.020	4.67 ± 0.11	0.490 ± 0.015	2.51 ± 0.06
	0.546 ± 0.030	5.14 ± 0.17	0.523 ± 0.015	2.60 ± 0.06
	0.549 ± 0.030	5.08 ± 0.25	0.552 ± 0.015	2.91 ± 0.08
	0.623 ± 0.023	5.48 ± 0.20	0.567 ± 0.015	2.83 ± 0.07
	0.666 ± 0.027	5.29 ± 0.18	0.648 ± 0.015	3.21 ± 0.09
	0.696 ± 0.038	5.53 ± 0.28	0.675 ± 0.015	3.20 ± 0.10
	0.775 ± 0.020	5.43 ± 0.20	0.687 ± 0.023	3.04 ± 0.10
	0.823 ± 0.033	5.31 ± 0.20	0.716 ± 0.015	3.63 ± 0.09
	0.843 ± 0.018	5.53 ± 0.14	0.719 ± 0.015	3.20 ± 0.13
	0.877 ± 0.038	5.37 ± 0.26	0.741 ± 0.015	3.47 ± 0.11

Appendix I *(cont.)*

Direction in the 001-plane. ($\alpha = 0° = [100]$-direction, $\alpha = 45° = [110]$-direction)	Longitudinal		Transverse	
	$q/q_{\max}$	$\omega \times 10^{-13}$ rad/sec	$q/q_{\max}$	$\omega \times 10^{-13}$ rad/sec
25° $q_{\max} = 1.712$ Å^{-1}	0.890 ± 0.035	5.37 ± 0.20	0.773 ± 0.020	3.40 ± 0.11
	0.902 ± 0.030	5.70 ± 0.23	0.885 ± 0.033	3.69 ± 0.17
	0.955 ± 0.030	5.15 ± 0.20	0.920 ± 0.015	3.53 ± 0.11
	0.967 ± 0.015	5.29 ± 0.18	0.936 ± 0.020	3.57 ± 0.11
	0.985 ± 0.021	5.30 ± 0.18		
30° $q_{\max} = 1.704$ Å^{-1}	0.298 ± 0.021	3.88 ± 0.11	0.182 ± 0.015	0.96 ± 0.03
	0.336 ± 0.015	3.69 ± 0.13	0.233 ± 0.015	1.45 ± 0.04
	0.373 ± 0.030	4.28 ± 0.16	0.242 ± 0.015	1.11 ± 0.03
	0.439 ± 0.015	4.74 ± 0.13	0.308 ± 0.015	1.48 ± 0.05
	0.462 ± 0.020	4.67 ± 0.11	0.370 ± 0.015	1.97 ± 0.04
	0.527 ± 0.035	5.06 ± 0.22	0.465 ± 0.015	2.44 ± 0.11
	0.545 ± 0.026	5.07 ± 0.25	0.474 ± 0.015	2.55 ± 0.07
	0.624 ± 0.018	5.39 ± 0.14	0.482 ± 0.015	2.52 ± 0.06
	0.648 ± 0.046	5.33 ± 0.26	0.523 ± 0.015	2.48 ± 0.06
	0.735 ± 0.041	5.61 ± 0.34	0.562 ± 0.015	2.64 ± 0.06
	0.770 ± 0.030	5.32 ± 0.21	0.567 ± 0.015	2.84 ± 0.07
	0.786 ± 0.015	5.57 ± 0.15	0.633 ± 0.015	2.97 ± 0.07
	0.886 ± 0.017	5.13 ± 0.19	0.639 ± 0.015	2.97 ± 0.18
	0.889 ± 0.033	5.30 ± 0.19	0.652 ± 0.015	2.92 ± 0.12
	0.902 ± 0.030	5.23 ± 0.18	0.652 ± 0.027	2.94 ± 0.12
	0.909 ± 0.035	5.60 ± 0.28	0.830 ± 0.023	3.45 ± 0.11
	0.989 ± 0.020	5.20 ± 0.14	0.833 ± 0.015	3.53 ± 0.16
			0.839 ± 0.015	3.53 ± 0.11
35° $q_{\max} = 1.671$ Å^{-1}	0.165 ± 0.031	1.86 ± 0.09	0.193 ± 0.015	0.97 ± 0.03
	0.309 ± 0.025	3.83 ± 0.12	0.215 ± 0.015	1.17 ± 0.04
	0.329 ± 0.022	3.74 ± 0.12	0.232 ± 0.015	1.23 ± 0.04
	0.372 ± 0.015	4.26 ± 0.10	0.233 ± 0.015	1.05 ± 0.03
	0.444 ± 0.017	4.72 ± 0.11	0.295 ± 0.015	1.40 ± 0.04
	0.453 ± 0.020	4.67 ± 0.13	0.479 ± 0.019	2.54 ± 0.07
	0.547 ± 0.031	5.01 ± 0.17	0.482 ± 0.015	2.49 ± 0.06
	0.552 ± 0.023	5.00 ± 0.17	0.488 ± 0.015	2.32 ± 0.08
	0.635 ± 0.017	5.34 ± 0.13	0.546 ± 0.020	2.82 ± 0.08
	0.648 ± 0.037	5.24 ± 0.21	0.607 ± 0.015	2.79 ± 0.14
	0.743 ± 0.015	5.57 ± 0.17	0.611 ± 0.015	2.78 ± 0.08
	0.774 ± 0.031	5.29 ± 0.20	0.705 ± 0.020	2.98 ± 0.12
	0.788 ± 0.036	5.22 ± 0.20	0.790 ± 0.015	3.26 ± 0.13
	0.876 ± 0.026	5.29 ± 0.24	0.791 ± 0.015	3.27 ± 0.08
	0.924 ± 0.023	5.18 ± 0.20	1.000 ± 0.033	3.70 ± 0.15
	0.941 ± 0.036	5.47 ± 0.24		
	0.946 ± 0.031	5.32 ± 0.18		
	0.978 ± 0.023	4.94 ± 0.13		
40° $q_{\max} = 1.652$ Å^{-1}	0.302 ± 0.016	3.84 ± 0.10	0.203 ± 0.016	1.02 ± 0.03
	0.320 ± 0.016	3.78 ± 0.12	0.219 ± 0.016	1.04 ± 0.03
	0.378 ± 0.016	4.25 ± 0.10	0.222 ± 0.016	1.24 ± 0.04
	0.445 ± 0.034	4.72 ± 0.18	0.231 ± 0.016	1.32 ± 0.04
	0.447 ± 0.016	4.73 ± 0.09	0.284 ± 0.016	1.39 ± 0.04
	0.555 ± 0.028	4.97 ± 0.18	0.477 ± 0.023	2.51 ± 0.10
	0.555 ± 0.028	4.98 ± 0.20	0.484 ± 0.023	2.49 ± 0.12
	0.644 ± 0.017	5.27 ± 0.12	0.531 ± 0.027	2.88 ± 0.13
	0.644 ± 0.028	5.23 ± 0.19	0.547 ± 0.027	2.83 ± 0.14

Appendix I *(cont.)*

Direction in the 001-plane. ($\alpha = 0° = [100]$-direction, $\alpha = 45° = [110]$-direction)	Longitudinal		Transverse	
	$q/q_{\max}$	$\omega \times 10^{-13}$ rad/sec	$q/q_{\max}$	$\omega \times 10^{-13}$ rad/sec
40° $q_{\max} = 1.652$ Å^{-1}	0.773 ± 0.039	5.29 ± 0.22	0.570 ± 0.016	2.64 ± 0.06
	0.778 ± 0.031	5.25 ± 0.19	0.594 ± 0.016	2.57 ± 0.14
	0.803 ± 0.036	5.51 ± 0.29	0.730 ± 0.016	3.09 ± 0.12
	0.864 ± 0.027	5.42 ± 0.26	0.734 ± 0.016	3.07 ± 0.07
	0.950 ± 0.025	5.31 ± 0.20	0.761 ± 0.016	3.07 ± 0.07
	0.961 ± 0.028	5.16 ± 0.23	0.931 ± 0.016	3.43 ± 0.07
	0.972 ± 0.044	5.12 ± 0.25		
45° $q_{\max} = 1.640$ Å^{-1}	0.165 ± 0.031	1.86 ± 0.09	0.213 ± 0.016	1.02 ± 0.03
	0.310 ± 0.024	3.82 ± 0.12	0.227 ± 0.016	1.28 ± 0.04
	0.445 ± 0.031	4.67 ± 0.18	0.483 ± 0.019	2.48 ± 0.10
	0.555 ± 0.028	4.95 ± 0.19	0.536 ± 0.016	2.57 ± 0.06
	0.643 ± 0.028	5.24 ± 0.18	0.539 ± 0.022	2.83 ± 0.09
	0.784 ± 0.031	5.22 ± 0.18	0.687 ± 0.016	2.92 ± 0.08
	0.843 ± 0.028	5.50 ± 0.25	0.845 ± 0.016	3.23 ± 0.07
	1.000 ± 0.028	5.31 ± 0.21		
	1.000 ± 0.038	5.10 ± 0.23		
	1.000 ± 0.044	5.08 ± 0.23		

APPENDIX II

Observed line widths δt_{obs} corresponding to $\delta \lambda_0$ in the text, and derived phonon line widths, δT, given in °K as a function of crystal temperature.

Transverse vibration

T°K	δt_{obs}	Line width	
		μsec	δT°K
293	135 ± 5		
593	140 ± 7	37 ± 29	12.3 ± 9.7
700	145 ± 7	53 ± 21	17.0 ± 6.7
793	152 ± 5	70 ± 13	22.0 ± 4.0
824	166 ± 5	97 ± 10	30.0 ± 3.0
854	171 ± 5	110 ± 9	34.0 ± 2.7
873	180 ± 5	119 ± 8.5	36.5 ± 2.6
882	176 ± 5	113 ± 9	35.0 ± 2.7
892	180 ± 5	119 ± 8.5	36.5 ± 2.6
903	180 ± 5	119 ± 8.5	36.3 ± 2.6
917	179 ± 5	118 ± 8.5	35.9 ± 2.6
923	182 ± 5	122 ± 8	37.0 ± 2.5
932	183 ± 5	124 ± 8	37.2 ± 2.5

Longitudinal vibration

T°K	δt_{obs}	Line width	
		µsec	δT°K
293	110		
820	125 ± 5	59 ± 13	25.8 ± 5.7
844	128 ± 5	65 ± 12	27.7 ± 5.1
882	137 ± 5	82 ± 10	34.5 ± 4.2
903	137 ± 5	82 ± 10	34.5 ± 4.2
916	140 ± 5	87 ± 10	36.7 ± 4.0
923	140 ± 5	87 ± 10	36.6 ± 4.0
932	141 ± 5	88 ± 9	37.0 ± 4.0

Tryckt den 1 april 1960

Uppsala 1960. Almqvist & Wiksells Boktryckeri AB